water

MDPI

Article

Infiltration and Short-Time Recharge in Deep Karst Aquifer of the Salento Peninsula (Southern Italy): An Observational Study

Marco Delle Rose and Paolo Martano *

CNR—Istituto di Scienze dell'Atmosfera e del Clima, U.O.S. Lecce, Via Monteroni, 73100 Lecce, Italy; m.dellerose@le.isac.cnr.it

* Correspondence: p.martano@isac.cnr.it; Tel.: +39-832-298718

Received: 21 December 2017; Accepted: 22 February 2018; Published: 2 March 2018

Abstract: Time series of micrometeorological data from the CNR ISAC-Lecce base have been used to estimate the seasonal/yearly surface infiltration in the period 2003–2016 in the Salento peninsula (Southern Italy). The estimated values of infiltration were compared with piezometric levels measured in the regional karst aquifer during the overlapping period 2009–2011. The results, besides the complex groundwater circulation, suggest the possibility of a quite short-time component in the deep aquifer response to the recharge input. This quick response, together with the growing hydroclimatic intensity, outlined in literature studies and observed in the last decade, could increasingly affect the seasonal aquifer dynamics in the near future. Some possible consequences on the water management in karst regions under Mediterranean climate are discussed.

Keywords: karst aquifer; surface hydrologic budget; infiltration; water resource management

1. Introduction

The modern management of water resources requires constant update to surface–subsurface hydrological interactions. Due to the uncertain effects of the climate change, it is essential to scrutinize the relation between precipitation, evapotranspiration, infiltration and runoff. Such an issue is pressing, especially in semi-arid and arid regions [1–3]. Concerning the renewable groundwater resources, the calculation of the net infiltration is crucial [4,5].

Among the various types of groundwater reservoirs, the karst aquifers receive special attention because they may be affected by enhanced qualitative and quantitative decline in short terms [6,7]. Reduction in precipitation coupled with increasing evapotranspiration could produce dramatic deficit in the water balance of karst areas [8,9]. Consequently, not surprisingly, artificial systems of aquifer recharge have been implemented in several karst basins [10–13].

Different methods to estimate evapotranspiration are used in the surface hydrologic balance computations. Among these, the Penman–Monteith model is considered one of the most well founded and reliable, because of its simple analytical formulation derived from basic physical principles [14]. It is often at the core of several used formulas, also recommended by the FAO, generally in the form of corrections to the "reference (potential) evapotranspiration", that is more easily computed [15–17]. However, questions have been raised about this procedure, and indeed in dry or semiarid environments, exposed to strong changes in humidity conditions such as the Mediterranean regions, its direct use appears to be somehow questionable [18–20]. Consequently, studies concerning long term measurements of evapotranspiration to be applied in the surface water balance assessment are of direct interest in the semi-arid environments of the Mediterranean area.

This paper attempts to experimentally test the relation between precipitation, evapotranspiration, infiltration and aquifer recharge in a semi-arid karst region, namely the central Mediterranean Salento

peninsula, Italy. The aim is to obtain observational estimations of the surface and net infiltration and of the aquifer recharge response, and explore the complexity of the processes involved in the karst hydrology, in the perspective to refine the conceptual model.

2. Study Area Description

The Salento peninsula is located at the end point of Apulia region, at the southeastern edge of Italy (Figure 1). It is a warm temperate region with dry-hot summer (*Csa* climate type [21]), mild-wet winters and about 650 mm of average annual rainfall in the last decades [22,23]. Similar to the whole Mediterranean area, it is highly responsive to climate variability, thus severe possible incoming effects on water resources, ecosystems and human health have been recently pointed out [24,25].

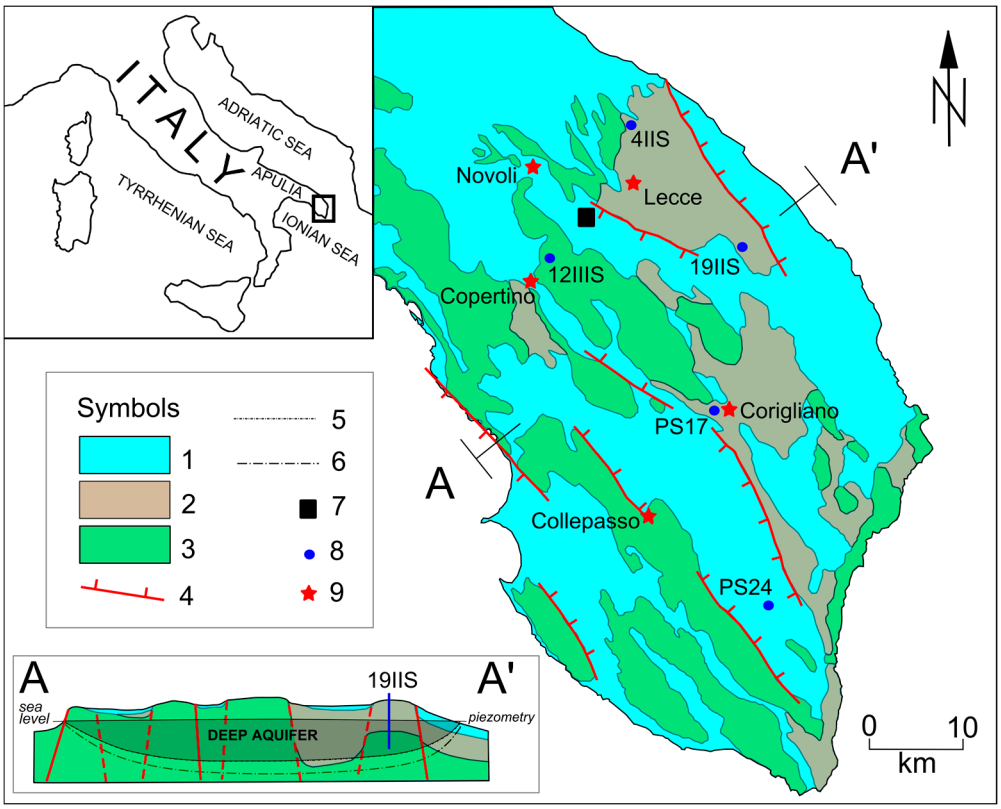

Figure 1. Location and geological map of Salento. Legend: **1**, coarse calcarenites and clayey-marls (Quaternary); **2**, fine calcarenites (Tertiary); **3**, limestone (Cretaceous); **4**, faults; **5**, fresh water/brackish water interface; **6**, brackish water/saltwater interface; **7**, CNR ISAC-Lecce micrometeorological base; **8**, selected wells of "progetto Tiziano"; and **9**, rain gauge stations of the Civil Protection Agency. Vertical scale magnified ten times in A–A′ section.

The peninsula is mainly exposed to northwesterly winds generally turning to southwesterly with approaching Atlantic lows. These latter, together with northeastern cold outbreaks, are responsible for most precipitating events. In addition, Mediterranean and local cyclogenesis, such as tropical-like-cyclones (TLCs or Medicanes) and supercell thunderstorm are not uncommon and likely to become increasingly stronger in the future [26,27]. The vegetation cover is characterized by Mediterranean scrub-land with several coastal pine forests and few residual oak woods, and agricultural areas with large extensions of olive groves and vineyards, and smaller irrigated patches of crops and orchards.

The Salento peninsula belongs to the Apulia Carbonate Platform, a crustal domain with a horst-and-graben tectonic arrangement. Lithologically, it is made up of limestones, calcarenites and clayey-marls (Figure 1). The horst (raised blocks) are constituted by Cretaceous limestone, while

Tertiary and Quaternary stratigraphic units cover the graben (lowered blocks). Due to the prevalence of carbonate rocks, landscape and substratum are characterized by karst forms. The geological setting strongly controls both the geomorphological and the hydrological features of the peninsula that shows, overall, a plateau, gently dipping from southeast (mean altitude 100 m a.s.l.) to northwest (mean altitude 35 m a.s.l.). The highest relief is almost at 200 m a.s.l. About three quarter of the territory has topographic gradients less than 1% and only one tenth has gradients around 3%. It does not show well defined watersheds. Drainage pattern is formed by several small systems of ephemeral rills and gullies that allow identifying both endorheic and exorheic basins [28]. Inside the former basins, karst landforms, such as dolines, sinkholes and crevices, act as swallow holes (terminology according to USEPA [29]). Previous studies estimated a typical runoff around 4% of the total water budget on a yearly base [17], possibly suggesting the effect of quick conduit-dominated infiltration [8,11]. In terms of pedology the Salento peninsula, together with central Apulia, form the "soil region" named "hills of Murge and Salento" that is dominated by well-drained humus-enriched soils (luvisol type), whereas both weak-developed mineral soils (regosol) and weak-differentiated soils (cambisol) are subordinated [30]. In term of water balance, the physical behavior of these terrains can be considered homogeneous at the kilometric scale.

Salento water reserves are stored in different aquifers. The main underground reservoir is a deep (regionally-extended) karst aquifer while the other groundwater bodies are local shallow aquifers. The first forms a complex aquifer system consisting in an unconfined predominant part laterally bounded by semi-confined parts according to the aforementioned horst-and-graben tectonic structure. It is mainly made up of Cretaceous limestones and contain a large lens of freshwater floating on salt water of continental intrusion [31] with a thick transition zone of variable saline content (see section A–A′ in Figure 1). Due to the wide range of variations of the main control factors, such as lithology changes, tectonic fractures development and karstification degree, the definition of the average hydraulic features is a hard issue for the deep aquifer. However, mathematical models may provide useful tools for the boundary conditions and the resource management [32]. The deep aquifer represents the only available drinking water resource in the region and currently provides about 75% of the demand. Where significant runoff is discharged in swallow karst holes, the hazard of a decrease of the groundwater quality due to an increase of intense rains has recently been emphasized [28].

Rainfall rapidly infiltrates from the Cretaceous outcrops into the deep aquifer due to the high permeability of the vadose zone, while it may take tens of years for the meteoric water to reach the shallow aquifers through the Tertiary and Quaternary rocks due to low permeability values [33]. However, the faults dissecting the tectonic blocks constitute hydraulic connections among the aquifers, thus allowing fast vertical drainage and complicating the conceptual hydrogeological model [34]. Nevertheless, the connection between the confined part of the deep aquifer and its unconfined parts is not yet well defined but seems to be largely influenced by layers with significant hydraulic conductivity in the horizontal direction [35]. The shallow aquifers may temporarily intercept most part of the effective infiltration and are mainly exploited in agriculture [36]. Groundwater flows in the shallow aquifers through both pores and dissolution-enlarged discontinuities. Inside the deep aquifer and the vadose zone, groundwater flows in tectonic fractures and sedimentary planes affected by karst dissolution throughout geological time. The geometry of the network is random and the width of the discontinuities ranges from a few millimeters up to several meters [37].

The current model of the deep aquifer inflows-outflows dynamics was conceptualized in a pioneer study of the 1950s and later confirmed [17,38]. The deep aquifer should recharge during the wet season (October–March), mainly by water percolated through Cretaceous limestone and Quaternary carbonate rocks (Figure 1), while no effective input is expected during the dry season.

3. Materials and Methods

This work analyzes and compares two datasets overlapping in a period of about three years (2009–2011). The first dataset was collected by the CNR ISAC micrometeorological base located

at 40°20′11.7″ N, 18°7′16.6″ E (Figure 1), which has been active for several years (2003–2017) in monitoring the surface water and energy balance in the area of Salento University Campus near Lecce, Italy (www.basesperimentale.le.isac.cnr.it). The CNR ISAC micrometeorological station consists of an eddy covariance system [39] on a 15-meter mast measuring turbulent vertical sensible heat flux H and water vapor (evapotranspiration) flux E, wind speed, air temperature and humidity. It is completed by an ancillary automatic meteorological station collecting long and short wave radiation (net radiation Rn), precipitation P, and soil data at two depths (temperature at 2 and 5 cm, soil heat flux G at 2 and 5 cm, and soil moisture at 2 and 35 cm underground). The data are stored as 30-min averages in the web database. More details about the base instruments, calibrations and the database can be found elsewhere [20,23,40].

Figure 2 shows the typical yearly distribution of the footprints of the scalar turbulent fluxes measured from the mast, calculated by the analytic model of Hsieh et al. [41]. They represent the distance from the mast that contributes to 90% of the measured evapotranspiration and heat fluxes (at 15 m height), which changes according to the local atmospheric conditions, and is a useful tool to assess the areal representativeness of the evapotranspiration measurements [39]. The histogram shows the yearly (2010) frequency distribution of the distances from the mast corresponding to the measured evapotranspiration flux (30-min averages) that has a 90% probability to be generated by the surface within the distance from the mast shown in the horizontal axis.

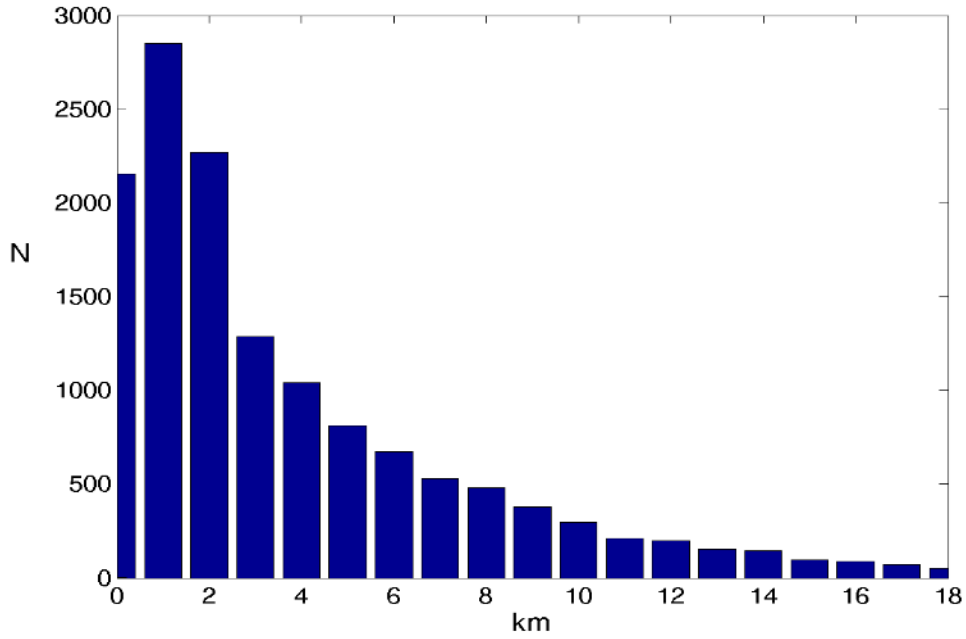

Figure 2. Frequencies N of the calculated 90% footprints in one year (2010), expressed as distances in km from the measurement mast, from 30-minute averaged data of the ISAC-Lecce database.

It appears that the measured evapotranspiration flux is representative of an area within about 2 km of the mast about 55% of the time, and between 2 km and 10 km for a residual 40%. Indeed, an area of a few square kilometers is also considered to be significant for surface rain gauge measurements cumulated in time, as well as in the worst case of localized convective precipitations, as space correlation generally tends to increase with the averaging time due to the translation of precipitating fronts over the measurement region and the averaging of local effects [42]. However, even over small regions such as the Salento peninsula precipitation can show some spatial patterns due to geographic and topographic reasons, spatially varying from about 550 to 800 mm per year over multi-decadal time scales [43,44]. The characteristic of the measurement area within 2 km from the ISAC base, covered by Mediterranean shrubs between olive groves and evergreen trees (mainly

pines), are typical of Salento. In addition, the lack of strongly evaporative surface hydrological basins inland, with only small patches of irrigated crops and few basins along the coast, should prevent the presence of large surface non-homogeneities in the evapotranspiration in Salento. Thus, the long-term precipitation/evapotranspiration data from the measurement area are assumed relatively representative of the region, considering the above limitations.

The second datasets comes from the "progetto Tiziano", a five-year governmental campaign of aquifer monitoring aimed to assess both the quantity and quality of groundwater. The institutional program allowed to optimize a well monitoring network that has improved the hydrogeological and hydro-geochemical knowledge. Raw data of the "progetto Tiziano" are available online (http://www.sit.puglia.it/portal/portale_cis). Piezometric levels are available for several wells at 1 cm resolution as daily averages. They were recorded by automatic instruments (half hour interval reading) on tens of wells located throughout the territory of the Apulia region. The data of the well closest to the ISAC base (12IIIS) has been considered in this study for comparison with the data acquired by the micrometeorological base. Moreover, a further analysis has been performed with the aid of four more wells (4IIS, 19IIS, PS17, and PS24, see Figure 1) whose time-series show best continuity characteristics in the overlapping period 2009–2011 (Supplementary Materials). The available piezometer series are raw data (affected by instrumental errors), and an inspection has been made to eliminate clearly wrong (out of reasonable scale) data. All selected piezometers measured the levels of the deep aquifer even if perforated from Tertiary or Quaternary rocks (see as an example 19IIS in A-A′ section of Figure 1).

In the present work, the data from the ISAC base are mainly used to attempt an experimental evaluation of the net infiltration when the soil storage contribution can be a significant part of the total groundwater storage, for a comparison with the piezometric levels. The net infiltration, also named effective infiltration, is the rate at which surface infiltration recharges the aquifers. It is also defined as the fraction of surface infiltration that reaches depths below where it cannot be removed by evapotranspiration processes. For this purpose, the following mass conservation equation has been used:

$$S(t + dt) = S(t) + P - E - I - R \quad (1)$$

where S(t) is the soil water content per square meter, and P, E, I and R are the total precipitation, actual evapotranspiration, net infiltration and runoff in the time interval dt, respectively. As discussed above, due to the climatic and geological characteristics of the region, the runoff term R has been neglected. In fact, the ISAC base is placed on a large sub-horizontal ground without any appreciable slope, thus no hydrographic pattern can be identified. Ponding waters are not observed in the base area, while small ponds last at most few days in the region. Then, the net infiltration I in the time interval dt has been estimated as:

$$I = P - E - S(t + dt) + S(t) \quad (2)$$

In Equation (2), P and E are directly derived from the measurements, while S(t) has been calculated approximating a total soil moisture content per square meter as:

$$S(t) = h[s_1(t) + s_2(t)]/2 \quad (3)$$

where s_1 and s_2 are the available soil moisture density measurements (in m^3/m^3 at 2 cm and 35 cm underground, respectively) and h represents an effective soil thickness, which has been determined as the value that minimizes the total possible negative output for I (varying h between 5 and 100 cm by a 5 cm step). The value of h = 40 cm found in this way has been then used in the final evaluations of I. The range of soil moisture content per square meter (0–160 mm) obtained with this value of h in Equation (3) is consistent with the range of variability observed in Salento maps of soil moisture content [17]. Equation (2) has been used at monthly and daily resolution in the following paragraphs.

To compare the variation in the measured piezometric levels with the net infiltration I between t and t+dt (Equation (2)), the difference of the piezometric levels, W, between t+dt and t has been calculated, for both single wells and averaged over different wells as mentioned in the following paragraphs. Finally, this has been used to calculate a cross-correlation function C(nt) for a time resolution t and an integer n (time-lag: nt) between I and W, defined as:

$$C(nt) = (1/N)\sum_{i=1}^{N}[I(t_i) - I][W(t_i + nt) - W] \quad (4)$$

where the sum $\sum$ over the index i is extended to all the available N couples of data $I(t_i)$ and $W(t_i+nt)$, and < > indicates the averaged value over the time series. C(nt) has then been normalized dividing by C(0).

4. Results

Some results from the 2003−2016 period of activity of the micrometeorological base concerning the surface water budget are shown in Table 1. They are the seasonal and yearly total values of measured precipitation (P), surface infiltration (T=P−E) and averaged values of surface soil moisture measured at 2 cm depth (soil moisture at 35 cm depth is not available before 2009). In these yearly/seasonal totals, the difference between precipitation and evapotranspiration may approximate the surface infiltration because of the negligible runoff.

Table 1. Total precipitation P, total surface infiltration (T=P−E, where E is evapotranspiration) and average surface soil moisture (measured at 2 cm depth), all averaged over the dry season, the wet season and the whole year in the period 2003–2016. The uncertainties represent the standard deviations in the 2003–2016 period. Data from the ISAC-Lecce database.

(2003–2016 Period)	Precipitation (m)	Surface Infiltration (m)	Soil Moisture (m/m)
Dry season (April–September)	0.25 ± 0.13	0.06 ± 0.13	0.11 ± 0.05
Wet season (October−March)	0.45 ± 0.13	0.33 ± 0.13	0.25 ± 0.05
Year	0.70 ± 0.13	0.39 ± 0.13	0.18 ± 0.05

The uncertainties represent the standard deviations of the seasonal values in the whole 2003–2016 period. Clearly, the year is split into two climatic seasons (warm-dry and mild-wet) according to the hydrological cycle. The seasonal variations of the average infiltration and soil moisture suggest the conventional approximation of considering a wet "recharge" season and a dry "deficit" season for the aquifers [38].

Figure 3 shows the seasonal T=P−E values for each year of measurements, whereby the two different seasonal hydrologic regimes are also quite clearly evident. (It also shows the calculated HY-INT index [45]—from the ISAC-Base data—for the dry season, mentioned in the Discussion). However, note the anomalous dry season infiltration in 2009–2010, which equals or even exceeds the wet season value.

Figure 4 shows the calculated net infiltration I as monthly totals in the study period 2009−2011 from Equation (2) and the surface infiltration T (T=P−E) for comparison. It appears that the soil storage acts as a "correction" from the surface to the net infiltration, which reduces the negative values for I, as expected, but without completely eliminating them. This is due to the inherent uncertainty in the soil moisture content evaluations from two points measurements, which are affected by a much smaller areal footprint with respect to evaporation/precipitation measurements (because of the very local soil non-homogeneities and variations in depth), and to the measurements error in E that appears to be, together with P, a main contribution in the evaluation of I. The soil storage contribution is expected to become less relevant as far as longer periods are concerned (year, season).

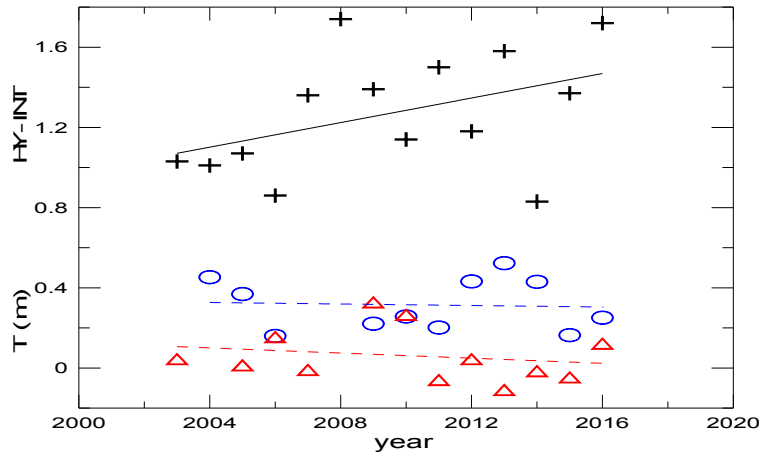

Figure 3. Surface infiltration (T=P−E) in the dry (April–September, red triangles) and wet (October–March, blue circles) season. Values in meters. Dashed lines are linear regressions. Seasonal HY-INT index (+) for the dry season (non-dimensional). The continuous line is a linear regression with a 90% confidence of increasing trend by the Mann–Kendall test.

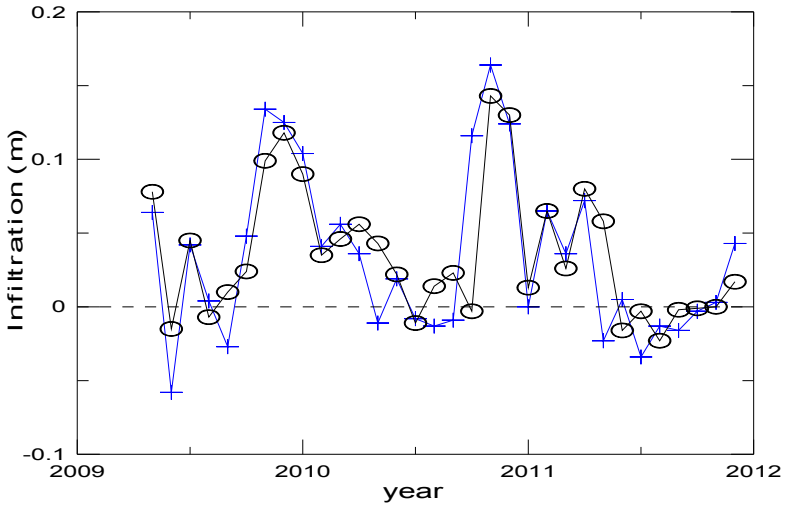

Figure 4. Surface infiltration T=P−E (+) and net infiltration I from Equation (2) (o) for the overlapping period of analysis (2009–2011). Values in meters. The continuous lines have been added for visual clarity only.

An estimate of the uncertainties in the measurements of E comes from Figure 5, which shows the measured total vertical turbulent energy flux (sum of sensible plus latent heat fluxes: H+λE, where λ is the evaporation latent heat) versus the measured surface available energy (net radiation minus surface soil heat fluxes: Rn-G), averaged daily. Due to energy conservation, they should perfectly match in measurements over an ideal surface [14], in the ideal case of only vertical transfer fluxes [39].

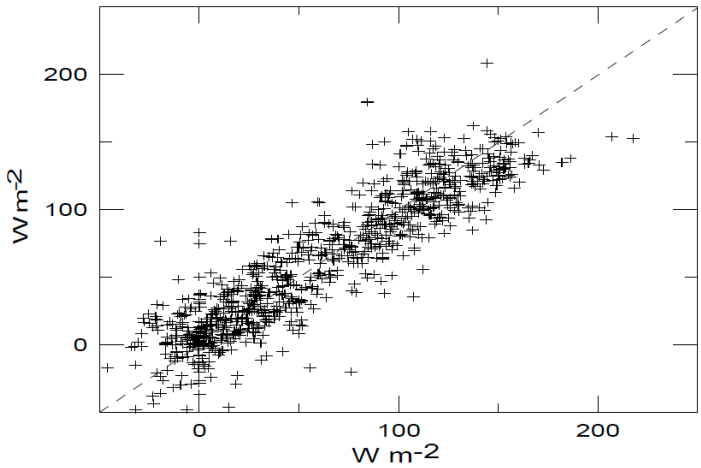

Figure 5. Sum of the sensible and latent heat fluxes (H+λE, daily averages, vertical axis) versus the available energy flux (net radiation minus soil heat flux: Rn-G, horizontal axis) for the 2009–2011 period. Data from the ISAC-Lecce database. All values in watts per square meter. Dashed line: x = y.

Figure 5 shows a good correlation with an unexplained variance around the x = y line of 19 W/m^2. Attributing half of the variance to the measured E flux, this translates into an uncertainty of about 0.02 mm per day (taking three standard deviations as maximum uncertainty). In the worst case of all errors summing up, it means about 0.6 mm per month. Considering a minimum of 0.2 mm error in the resolution of the rain gauge, we have a minimum uncertainty of the order of 1 mm per month in the infiltration estimation, apart from the soil storage correction. However, the uncertainty can be quite large due to the missing data in the considered period. An estimation of the total measurement uncertainty considering both instrumentation errors and missing data has been suggested in [23], where the missing data uncertainty was estimated as proportional to both the contribution of the single measurement error and the total number of missing data (the total number of missing data per year is always less than 10%). The seasonal/yearly average/total values for P,I, and soil moisture at 2 cm in the short study period 2009–2011 are shown in Table 2, where the error interval now represents the total estimated measurement uncertainty from [23] (not the "climatic" standard deviation of the whole 2003–2016 period as in the long term averages of Table 1).

Table 2. Total precipitation P, total net infiltration (I from Equation (2)) and average surface soil moisture (measured at 2 cm depth), all averaged over the dry season, the wet season and the whole year in the overlapping period 2009–2011. The uncertainties take into account the measurement errors and the missing data. Data from the ISAC-Lecce database.

(2009–2011 Period)	Precipitation (m)	Net Infiltration (m)	Soil Moisture (m/m)
Dry season (April–September)	0.36 ± 0.04	0.12 ± 0.04	0.14 ± 0.04
Wet season (October–March)	0.36 ± 0.02	0.28 ± 0.02	0.23 ± 0.04
Year	0.72 ± 0.06	0.40 ± 0.06	0.19 ± 0.04

The short study period shows indeed some peculiarities with respect to the longer averages of Table 1. The difference between dry and wet season are less stringent and this is due to the evidence of significant precipitation events during the warm season 2009 and 2010 that can cause uncommonly relevant infiltration conditions (compare the dry season infiltration of Tables 1 and 2). Uncommon dry season infiltration in 2009–2010 is also evident from both in Figures 3 and 4.

Figure 6 shows plots of the measured 2009–2011 monthly piezometric differences W in the well 12IIIS (see Figure 1 for the location) versus the total monthly infiltration I from the ISAC base, respectively, with a time lag of 0–3 months between them.

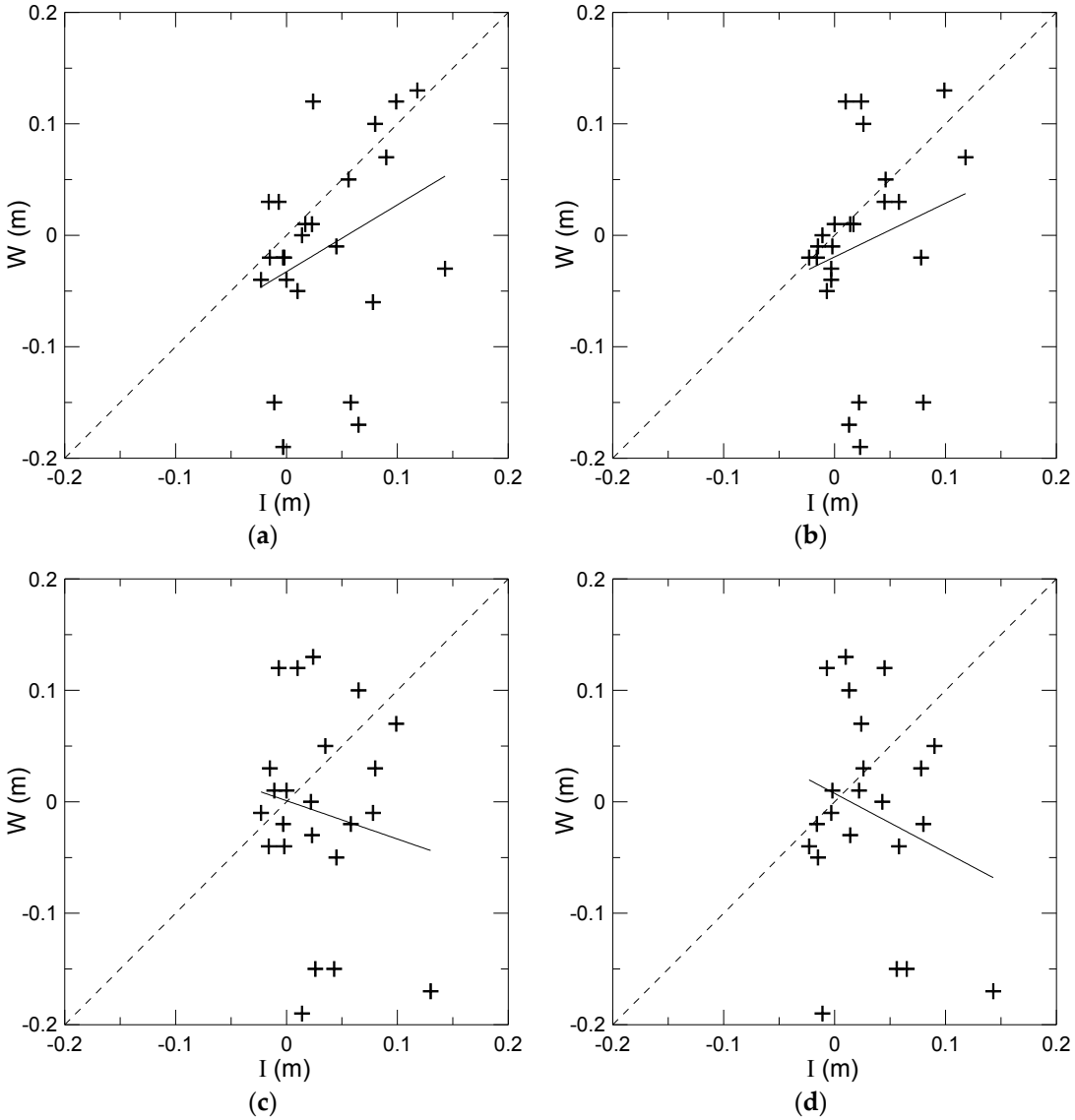

Figure 6. The 2009–2011 monthly variations in the piezometric level of well 12IIIS W versus total monthly infiltration I calculated by Equation (2) in: (**a**) the same month; (**b**) one month before; (**c**) two months before; and (**d**) three months before. All values in meters. The continuous lines are linear regressions, the dashed lines represent x = y.

The complexity of the aquifer inflows-outflows dynamics is evident from the figures, where, in addition to the majority of points being below the x = y line, which can be expected in wells affected by irrigation drainages and local discharge due to the aquifer dynamics, there are also a few points above the middle line that may correspond to water inputs besides the (local) net infiltration. However, even if some preliminary inspection to the time series allowed to exclude few clearly erroneous points (reasonably out of scale), measurement errors in the raw data of the well levels cannot be completely excluded.

The continuous lines in Figure 6 correspond to a linear regression. It shows that the correlation between the piezometric level increases and the local infiltration decreases with increasing time lag, suggesting a maximum correlation within the average period of one month.

To achieve a better validation of these results, the same comparison has been made using the averaged increases of the five wells shown in Figure 1 instead of just the single closest well. The results, shown in Figure 7, are qualitatively similar to Figure 6, with an expected reduced spread of the data, showing again a decrease of the correlation together with an increase of the number of points above the x = y line as the time lag increases.

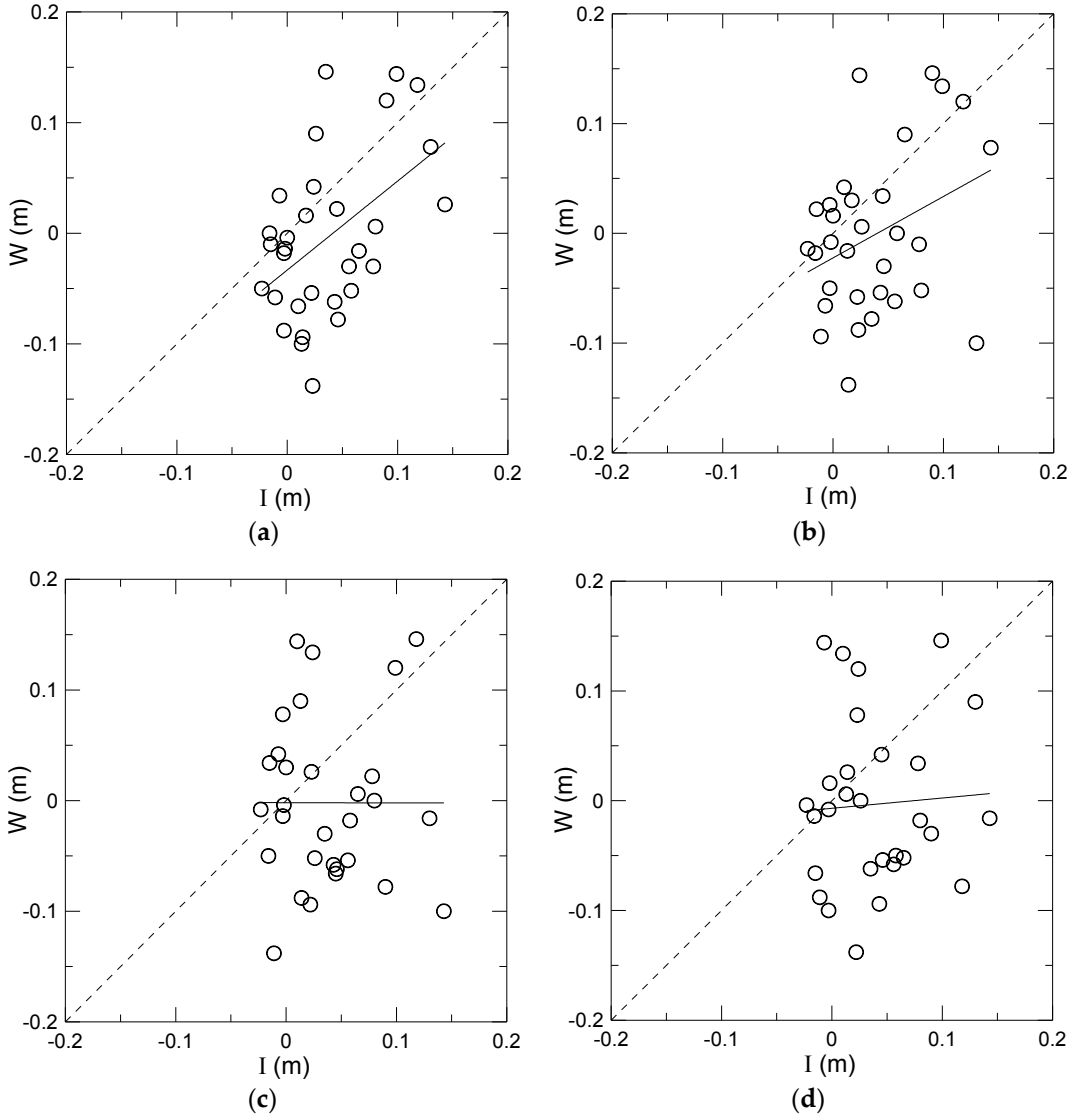

Figure 7. The 2009–2011 monthly variations in the averaged piezometric levels of all five wells W versus total monthly infiltration I calculated by Equation (2) in: (**a**) the same month; (**b**) one month before; (**c**) two months before; and (**d**) three months before. All values in meters. The continuous lines are linear regressions, the dashed lines represent x = y.

These results suggested a further analysis of the correlation between the infiltration I and the piezometric level variations W in the wells. Thus, the cross-covariance function C(nt) between I and W has been constructed using the whole available data series at 1-day time resolution (Equation (4)).

Figures 8 and 9 show the normalized C(nt) for the well 12IIIS and the averaged five wells of the "progetto Tiziano", respectively, both considering just the calculated I from Equation (2),

and the corrected I obtained substituting with zero the remaining negative values, for comparison. This function always evidences a short-term peak with maximum at about two days lag (n = 2, t = 1 day) and width of a few days for the closest well, with expected strong oscillations for longer time lags, but just around the zero value.

For the five wells averaged W in Figure 9, C(nt) is very similar to that reported in Figure 8, with an even clearer maximum in the same position, evidenced by a less noisy residual oscillation around zero.

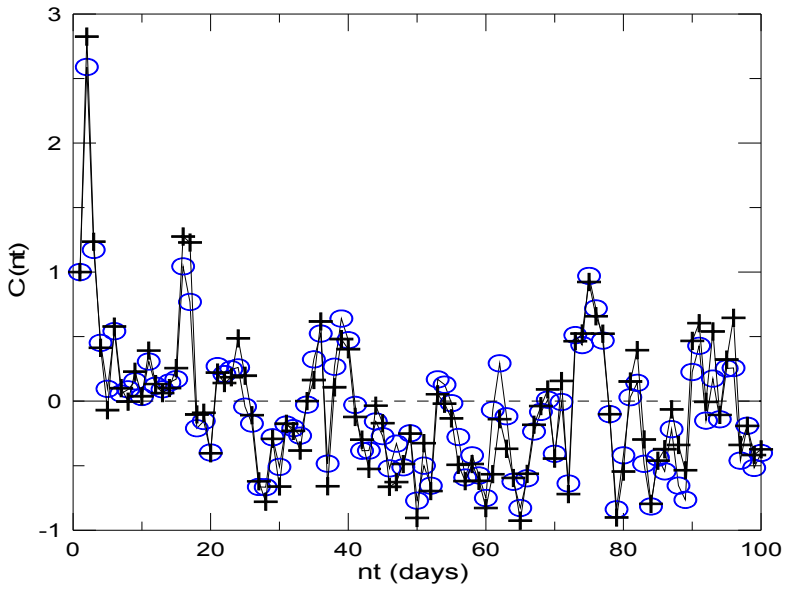

Figure 8. Cross-covariance functions C(nt) between the daily increments in the piezometric level for the closest well 12IIIS and daily net infiltration as calculated by Equation (2) (+), and corrected by vanishing negative values (o). Continuous lines added for visual clarity.

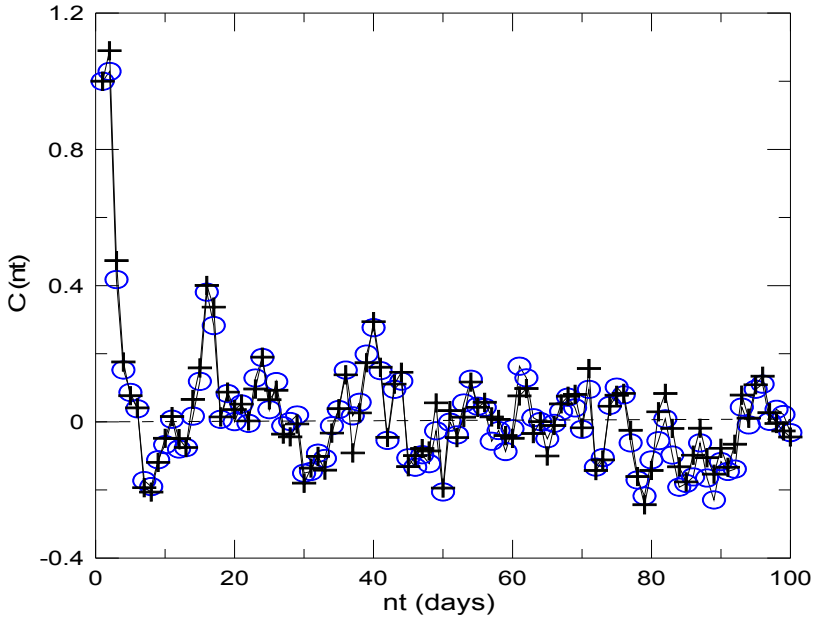

Figure 9. Same of Figure 8, but for the averaged piezometric increments of all the wells.

5. Discussion

5.1. Estimations of the Seasonal/Yearly Net Infiltration

The analysis of both the micrometeorogical data from the ISAC-Lecce database and some data series from selected wells from "progetto Tiziano" in the period 2009–2011 allowed assessing an evaluation of the infiltration and a comparison with the variations in the piezometric levels. The infiltration estimates were obtained from directly measured precipitation, evapotranspiration and soil moisture data that can be representative of a small but characteristic area of the Salento peninsula. This analysis suggests a small contribution of the soil storage over the total infiltration over medium to long periods (months, seasons, and years). The analysis of the results for the years 2009–2010, compared with the 2003–2016 average, also suggests that relevant precipitation events may provide net infiltration even during the dry season.

5.2. Infiltration, Precipitation Distribution and Aquifer Recharge

The comparison of the two datasets outlined the complexity of the processes governing the local changes in the aquifer level that made possible only a reliability assessment of the infiltration estimation and its correlation with the observed piezometric levels at different time lags. However, the cross-covariance analysis seems to confirm the presence of a short-time component (days) in the aquifer recharge from the local net infiltration, as suggested by previous studies [33,34].

Due to the restricted spatial variability of the precipitation over Salento Peninsula [43,44], Figures 7 and 9 might provide a clue on the recharge time delay at regional scale. The monthly precipitations over the Salento peninsula during the 2009–2011 are shown in Figure 10. The graph is elaborated according to pluviometry data of the rain gauges, belonging to the network of the Civil Protection Agency, located close to the "progetto Tiziano" wells [46–48].

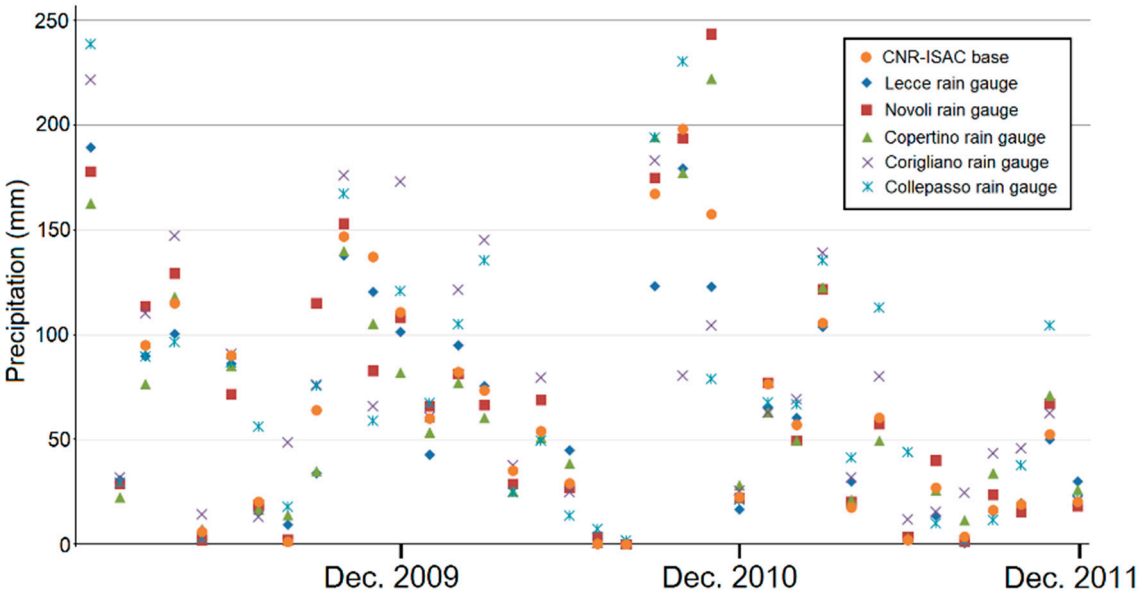

Figure 10. The 2009–2011 monthly precipitations (mm) measured at CNR-ISAC base and five selected rain gauges of the regional Civil Protection network.

In detail, the records of the rain gauges of Lecce, Novoli and Copertino, located at 5, 6.5 and 8.5 km from the CNR-ISAC micrometeorological base, respectively, are similar to the record of the base itself with few differences during October–November 2010. The records of rain gauges of Corigliano and Collepasso, located 23 and 30 km south of the base, respectively (Figure 1), reproduce the fluctuations of the reference record magnifying some rainfall peaks. This pattern of precipitation on the Salento

peninsula is also apparent at the daily scale. For example, Figure 11 shows the daily precipitations measured during the wet December 2009 at the five rain gauges here considered together with those measured at the CNR-ISAC base.

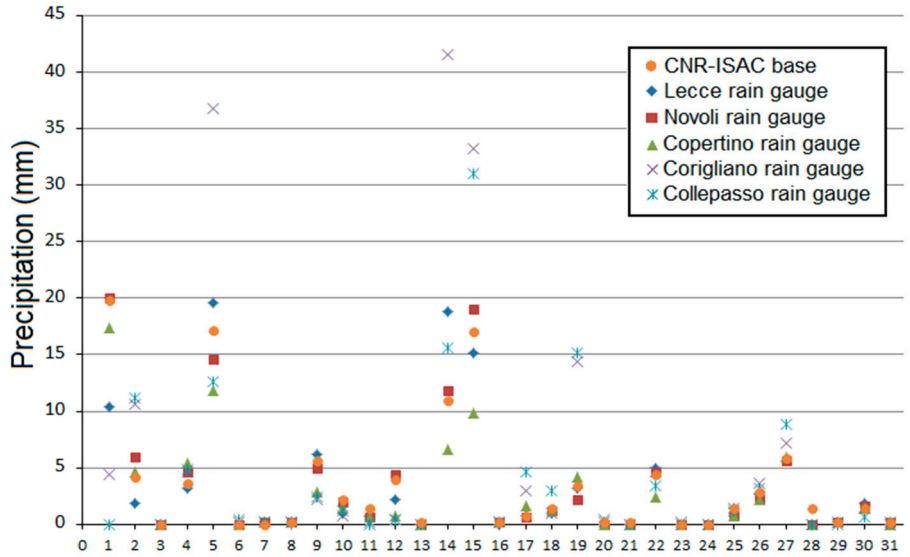

Figure 11. December 2009 daily precipitations (mm) measured at CNR-ISAC base and five selected rain gauges of the regional Civil Protection network.

A further example is in Figure 12 for the dry month June 2010, elaborated by data of the six rain gauges already considered.

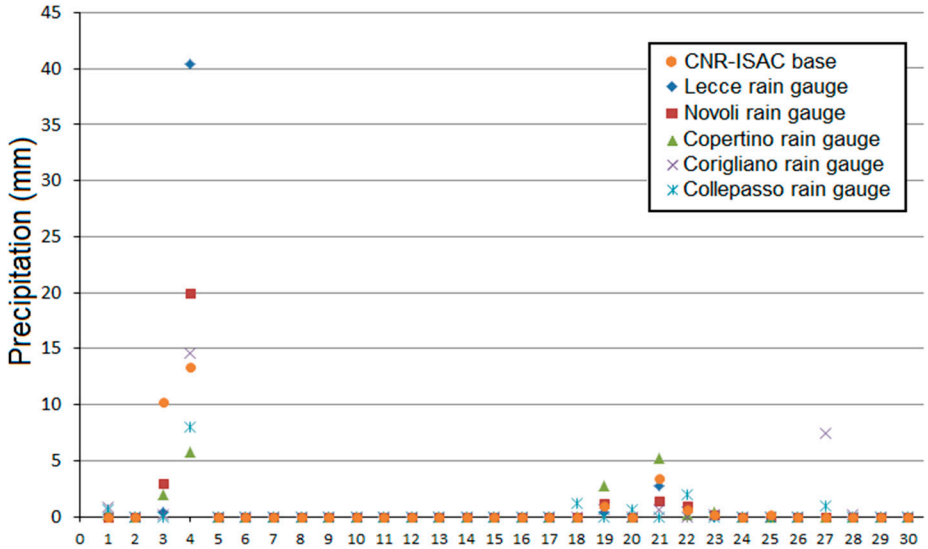

Figure 12. June 2010 daily precipitations (mm) measured at CNR-ISAC base and five selected rain gauges of the regional Civil Protection network.

It is to be noticed that the presence of a short-time recharge in the deep aquifer makes it directly sensitive to strong short-time hydrometeorological phenomena. An increasing of short but significant precipitation events separated by long totally dry spells has been shown as an almost ubiquitous signature of the global climate of the last decades by Giorgi et al. [45], who proposed an "ad hoc" hydroclimatic intensity index (HY-INT) to quantify it. This index is proportional to both the amount

of precipitation in wet days (days with P > 1 mm) and the average length of the dry spells (number of consecutive days with P < 1 mm) in the considered period of time, thus increasing with both the increasing "concentration" of precipitation events and the increasing of the length of the dry periods. Focusing over the Apulia region, some local climate projections by statistical downscaling found a possible increasing of local precipitation events in the warm season for the next decades [49]. In addition to the infiltration effects of the 2009–2010 dry seasons hydrological extremes, Figure 3 also shows the HY-INT index calculated for the dry seasons of the period 2003–2016 from the data of the ISAC-Lecce database, normalized by the averaged value of the same period. This evidences an increasing trend (at 90% confidence in the Mann–Kendall test), implying increasing significant short precipitation events among long very dry spells in the last decade. It should be remarked that the combination of the evidenced short-time recharge component and significant high hydroclimatic intensity phenomena, which are expected to keep increasing in the next decades, can directly affect and modify the average seasonal recharge dynamics of the deep aquifer, and should be considered in studies concerning the aquifer modelling and management. Consequently, the conceptual model of exclusive aquifer recharge in the wet season only should be revised.

5.3. Water Management Concerns

In an incoming Mediterranean climate scenario with increase of extreme rain events coupled with the decrease of annual rainfall [50], the water quality of karst aquifers may also be affected. In fact, short-time recharge events will predictably grow the sensitivity of these reservoirs also to short-lived contaminants because the fast travel times in the karst conduit of the vadose zone will further minimize adsorption, degradation, and filtration processes [7]. This should mainly affect karst catchments with significant percentage of both runoff and concentrated infiltration, as documented in the literature for several Apulia basins [51,52]. Severe consequences could also affect basins where runoff mixed with treated wastewater is drained toward karst swallow holes by systems of channels for managed aquifer recharge [10,12] such as the Asso Torrent basin of the Salento peninsula [28]. Here, the recharge is concentrated in a limited portion of the vadose zones, thus the dilution of the contaminants is also completely inhibited. Therefore, water authorities and managers will possibly face challenges on improving the quality of infiltration waters.

Supplementary Materials: The following are available online at www.mdpi.com/2073-4441/10/3/260/s1, Figure S1: Measured local precipitation and piezometric levels.

Acknowledgments: One of the authors (Martano) wishes to strongly acknowledge C. Elefante and F. Grasso for their fundamental help in the construction and maintenance of the ISAC-Lecce database (www.basesperimentale.le.isac.cnr.it). Raw data of the "progetto Tiziano" are available at http://www.sit.puglia.it/portal/portale_cis. The rain gauges data of the Civil Protection Agency of Apulia are available at http://www.protezionecivile.puglia.it/centro-funzionale. This work is a contribution to HyMeX program, with the partial support of the Italian PON I-AMICA. Publication fees supported by the "eartH_2Observe" project, funded by the European Union's Seventh Framework Program.

Author Contributions: Paolo Martano conceived, designed and performed the measurement at the ISAC base; Marco Delle Rose selected wells data; Marco Delle Rose and Paolo Martano analyzed the data and wrote the paper.

Conflicts of Interest: The authors declare no conflict of interest.

References

1. Green, T.R.; Taniguchi, M.; Kooi, H.; Gurdak, J.J.; Allen, D.M.; Hiscock, K.M.; Treidel, H.; Aureli, A. Beneath the surface of global change: Impacts of climate change on groundwater. *J. Hydrol.* **2011**, *405*, 532–560. [CrossRef]
2. Taylor, R.G.; Scanlon, B.; Döll, P.; Rodell, M.; van Beek, R. and others 21 authors. Ground water and climate change. *Nat. Clim. Chang.* **2012**, *3*, 322–329. [CrossRef]
3. Ries, F.; Lange, J.; Schmidt, S.; Puhlmann, H.; Sauter, M. Recharge estimation and soil moisture dynamics in a Mediterranean, semi-arid karst region. *Hydrol. Earth Syst. Sci.* **2015**, *19*, 1439–1456. [CrossRef]

4. Jemcov, I.; Petric, M. Measured precipitation vs. effective infiltration and their influence on the assessment of karst systems based on results of the time series analysis. *J. Hydrol.* **2009**, *379*, 304–314. [CrossRef]
5. Robertson, W.M.; Sharp, J.M. Estimates of net infiltration in arid basins and potential impacts on recharge and solute flux due to land use and vegetation change. *J. Hydrol.* **2015**, *522*, 211–227. [CrossRef]
6. Bonacci, O. Hazards caused by natural and anthropogenic changes of catchment area in karst. *Nat. Hazards Earth Syst. Sci.* **2004**, *4*, 655–661. [CrossRef]
7. Butscher, C.; Huggenberger, P. Modeling the Temporal Variability of karst groundwater vulnerability with implications for climate change. Environ. *Sci. Technol.* **2009**, *43*, 1665–1669. [CrossRef]
8. Hartmann, A.; Goldscheider, N.; Wagener, T.; Lange, J.; Weiler, M. Karst water resources in a changing world: Review of hydrological modeling approaches. *Rev. Geophys.* **2014**, *52*, 218–242. [CrossRef]
9. Neves, M.C.; Costa, L.; Monteiro, J.P. Climatic and geologic controls on the piezometry of the Querença-Silves karst aquifer, Algarve (Portugal). *Hydrogeol. J.* **2016**, *24*, 1015–1028. [CrossRef]
10. Page, D.; Dillon, P.; Vanderzalm, J.; Toze, S.; Sidhu, J.; Barry, K.; Levet, K.; Kremer, S.; Regel, R. Risk assessment of aquifer storage transfer and recovery with urban stormwater for producing water of a potable quality. *J. Environ. Qual.* **2010**, *39*, 2029–2039. [CrossRef] [PubMed]
11. Somaratne, N. Characteristics of point recharge in karst aquifers. *Water* **2014**, *6*, 2782–2807. [CrossRef]
12. Bacchus, S.T.; Bernardes, S.; Xu, W.; Madden, M. Fractures as Preferential Flowpaths for Aquifer Storage and Recovery (ASR) Injections and Withdrawals: Implications for Environmentally Sensitive Near-Shore Waters, Wetlands of the Greater Everglades Basin and the Regional Karst Floridan Aquifer System. *J. Geogr. Geol.* **2015**, *7*, 117–155. [CrossRef]
13. Xanke, J.; Jourde, H.; Liesch, T.; Goldscheider, N. Numerical long-term assessment of managed aquifer recharge from a reservoir into a karst aquifer in Jordan. *J. Hydrol.* **2016**, *540*, 603–614. [CrossRef]
14. Garratt, J.R. *The Atmospheric Boundary Layer*; Cambridge University Press: Cambridge, UK, 1992; 316p, ISBN 0-521-38052-9.
15. Federer, C.A.; Vorosmarty, C.; Fekete, B. Intercomparison of methods for calculating potential evaporation in regional and global water balance models. *Water Resour. Res.* **1996**, *32*, 2315–2321. [CrossRef]
16. Allen, R.G.; Pereira, L.S.; Raes, D.; Smith, M. *Crops Evapotranspiration: Guidelines for Computing Crop Water Requirements*; FAO Irrigation and Drainage Paper 56; FAO: Rome, Italy, 1998; 300p.
17. Portoghese, I.; Uricchio, V.; Vurro, M. A GIS tool for hydrogeological water balance evaluation on a regional scale in semi-arid environments. *Comput. Geosci.* **2005**, *31*, 15–27. [CrossRef]
18. Katerji, N.; Rana, G. FAO-56 methodology for determining water requirement of irrigated crops: Critical examination of the concepts, alternative proposals and validation in Mediterranean region. *Theor. Appl. Climatol.* **2014**, *115*, 515–536. [CrossRef]
19. Rana, G.; Katerji, N. Measurement and estimation of actual evapotranspiration in the field under Mediterranean climate: A review. *Eur. J. Agron.* **2000**, *13*, 125–153. [CrossRef]
20. Martano, P. Evapotranspiration Estimates over Non-Homogeneous Mediterranean Land Cover by a Calibrated "Critical Resistance" Approach. *Atmosphere* **2015**, *6*, 255–272. [CrossRef]
21. Peel, M.C.; Finlayson, B.L.; McMahon, T.A. Updated world map of the Köppen-Geiger climate classification. *Hydrol. Earth Syst. Sci.* **2007**, *11*, 1633–1644. [CrossRef]
22. Zito, G.; Ruggiero, L.; Zuanni, F. Aspetti meteorologici e climatici della Puglia. In Proceedings of the First Workshop on "Clima, Ambiente e Territorio nel Mezzogiorno", Taormina, Italy, 11–12 December 1989; CNR: Roma, Italy, 1991; pp. 43–73. (In Italian)
23. Martano, P.; Elefante, C.; Grasso, F. Ten years water and energy surface balance from the CNR-ISAC micrometeorological station in Salento peninsula (southern Italy). *Adv. Sci. Res.* **2015**, *12*, 121–125. [CrossRef]
24. Giorgi, F.; Lionello, P. Climate change projections for the Mediterranean region. *Glob. Planet. Chang.* **2008**, *63*, 90–104. [CrossRef]
25. Ladisa, G.; Todorovic, M.; Trisorio Liuzzi, G. A GIS-based approach for desertification risk assessment in Apulia region, SE Italy. *Phys. Chem. Earth* **2012**, *49*, 103–113. [CrossRef]
26. Gianfreda, F.; Miglietta, M.M.; Sansò, P. Tornadoes in Southern Apulia (Italy). *Nat. Hazards* **2005**, *34*, 71–89. [CrossRef]
27. Romera, R.; Gaertner, M.A.; Sánchez, E.; Domínguez, M.; González-Alemá, J.J.; Miglietta, M.M. Climate change projections of medicanes with a large multi-model ensemble of regional climate models. *Glob. Planet. Chang.* **2017**, *151*, 134–143. [CrossRef]

28. Delle Rose, M.; Fidelibus, C. Water resource management in karstic catchments: The case of the Asso Torrent basin (Southern Italy). *Environ. Earth Sci.* **2016**, *75*, 892. [CrossRef]
29. USEPA. *A Lexicon of Cave and Karst Terminology with Special Reference to Environmental Karst Hydrology (EPA/600/R-02/003)*; USEPA: Washington, DC, USA, 2002; 214p.
30. Costantini, E.A.C.; Barbetti, R.; Fantappiè, M.; L'Abate, G.; Lorenzetti, R.; Magini, S. Pedodiversity. In *The Soils of Italy*; Costantini, E.A.C., Dazzi, C., Eds.; Springer: Dordrecht, The Netherlands, 2013; pp. 105–178. [CrossRef]
31. Tadolini, T.; Tulipano, L. The evolution of fresh-water/salt-water equilibrium in connection with withdrawals from coastal carbonate and karstic aquifer of the salentine peninsula. *Geol. Jaharb.* **1981**, *29*, 69–85.
32. Carotenuto, L.; Di Pillo, G.; Raiconi, G.; Troisi, S. Mathematical modelling and parameter identification for a coastal aquifer. *Adv. Water Resour.* **1980**, *3*, 151–157. [CrossRef]
33. Delle Rose, M. Geological constraints on the location of industrial waste landfills in Salento karst areas (southern Italy). In *Water Pollution VI, Modelling, Measuring and Prediction*; Brebbia, C.A., Ed.; Witpress: Southampton, UK, 2001; pp. 57–68. ISBN 1-85312-878-3.
34. Tulipano, L. Temperature logs interpretation for the identification of preferential flow pathway in the coastal carbonatic and karstic aquifer of the Salento peninsula (southern Italy). In Proceedings of the 21st Congress of International Association of Hydrogeologists, Guilin, China, 10–15 October 1988; Volume 2, pp. 956–961.
35. Tadolini, T.; Tazioli, G.S.; Tulipano, L. Idrogeologia della zona delle sorgenti Idume (Lecce). *Geol. Appl. Idrogeol.* **1971**, *4*, 41–63. (In Italian)
36. Delle Rose, M. Sedimentological features of the plio-quaternary aquifers of Salento (Puglia). *Mem. Descr. Carta Geol. Ital.* **2007**, *76*, 137–146.
37. Delle Rose, M.; Federico, A.; Fidelibus, C. A computer simulation of groundwater salinization risk in Salento peninsula (Italy). In *Risk Analysis II*; Brebbia, C.A., Ed.; Witpress: Southampton, UK, 2000; pp. 465–475. ISBN 1-85312-830-9.
38. Cotecchia, V. Sviluppi della teoria di Ghyben ed Herzberg nello studio idrogeologico dell'alimentazione e dell'impiego delle falde acquifere, con riferimento a quella profonda delle Murge e del Salento. *Geotecnica* **1958**, *6*, 301–318. (In Italian)
39. Aubinet, M.; Vesala, T.; Papale, D. (Eds.) *Eddy Covariance. A Practical Guide to Measurement and Data Analysis*; Springer: Dordrecht, The Netherlands, 2012. [CrossRef]
40. Martano, P.; Elefante, C.; Grasso, F. A database for long term atmosphere-surface transfer monitoring in Salento Peninsula (Southern Italy). *Dataset Papers Geosci.* **2013**, 946431. [CrossRef]
41. Hsieh, C.I.; Katul, G.G.; Chi, T.W. An approximate analytical model for footprint estimation of scalar fluxes in thermally stratified atmospheric flows. *Adv. Water Resour.* **2000**, *23*, 765–772. [CrossRef]
42. Kidd, C.; Becker, A.; Huffman, G.J.; Muller, C.L.; Joe, P.; Skonfronick-Jackson, G.; Kirchbaum, D. So, how much of the Earth's surface is covered by rain gauges? *Bull. Am. Meteorol. Soc.* **2017**, *98*, 69–78. [CrossRef]
43. Carrozzo, M.T.; Delle Rose, M.; De Marco, M.; Federico, A.; Forte, F.; Margiotta, S.; Negri, S.; Pennetta, L.; Simeone, V. Pericolosità di allagamento nel Salento leccese. *Ital. J. Eng. Geol. Environ.* **2003**, *2*, 77–85.
44. Forte, F.; Pennetta, L.; Strobl, R.O. Historic records and GIS applications for flood risk analysis in the Salento peninsula (Southern Italy). *Nat. Hazards Earth Syst. Sci.* **2005**, *5*, 833–844. [CrossRef]
45. Giorgi, F.; Im, E.S.; Coppola, E.; Diffenbaugh, N.S.; Gao, X.J.; Mariotti, L.; Shi, Y. Higher Hydroclimatic Intensity with Global Warming. *J. Clim.* **2011**, *24*, 5309–5324. [CrossRef]
46. Regione Puglia. Annali Idrologici. 2009. Available online: http://www.protezionecivile.puglia.it/wp-content/uploads/Annali_I/annale2009.pdf (accessed on 30 November 2017). (In Italian)
47. Regione Puglia. Annali Idrologici. 2010. Available online: http://www.protezionecivile.puglia.it/wp-content/uploads/Annali_I/annale2010.pdf (accessed on 30 November 2017). (In Italian)
48. Regione Puglia. Annali Idrologici. 2011. Available online: http://www.protezionecivile.puglia.it/wp-content/uploads/Annali_I/annale2011.pdf (accessed on 30 November 2017). (In Italian)
49. Palatella, L.; Miglietta, M.M.; Paradisi, P.; Lionello, P. Climate change assessment for Mediterranean agricultural areas by statistical downscaling. *Nat. Hazards Earth Syst. Sci.* **2010**, *10*, 1647–1661. [CrossRef]
50. Alpert, P.; Ben-Gai, T.; Baharad, A.; Benjamini, Y.; Yekutieli, D.; Colacino, M.; Diodato, L.; Ramis, C.; Homar, V.; Romero, R.; et al. The paradoxical increase of Mediterranean extreme daily rainfall in spite of decrease in total values. *Geophys. Res. Lett.* **2002**, *29*. [CrossRef]

51. Fidelibus, M.D.; Balacco, G.; Gioia, A.; Iacobellis, V.; Spilotro, G. Mass transport triggered by heavy rainfall: The role of endorheic basins and epikarst in a regional karst aquifer. *Hydrol. Process.* **2017**, *31*, 394–408. [CrossRef]
52. Miglietta, P.P.; Toma, P.; Fanizzi, F.P.; De Donno, A.; Coluccia, B.; Migoni, D.; Bagordo, F.; Serio, F. A Grey Water Footprint Assessment of Groundwater Chemical Pollution: Case Study in Salento (Southern Italy). *Sustainability* **2017**, *9*, 799. [CrossRef]